Inorg. Chem. **2005**, *44*, 3389–3395

Magnetic Polyoxometalates: Anisotropic Exchange Interactions in the Co^{II}_3 Moiety of $[(NaOH_2)Co_3(H_2O)(P_2W_{15}O_{56})_2]^{17-}$

Juan Modesto Clemente-Juan,*,† Eugenio Coronado,† Alejandro Gaita-Ariño,† Carlos Giménez-Saiz,† Hans-Ulrich GUdel,‡ Andreas Sieber,‡ Roland Bircher,‡ and Hannu Mutka§

Instituto de Ciencia Molecular, Universitat de València, c/ Dr. Moliner, 50 46100 Burjassot, Spain, Department of Chemistry and Biochemistry, Universität Bern, Freiestrasse, 3, 3000 Bern 9, Switzerland, and Institut Laue Langevin, Avenue des Martyrs, B.P. 156, 38042 Grenoble, Cedex 9, France

Received October 15, 2004

The magnetic exchange interactions in a Co^{II}_3 moiety encapsulated in Na_{17} $[(NaOH_2)Co_3(H_2O)(P_2W_{15}O_{56})_2]$ (**NaCo**$_3$) were studied by a combination of magnetic measurements (magnetic susceptibility and low-temperature magnetization), with a detailed Inelastic Neutron Scattering (INS) investigation. The novel structure of the salt was determined by X-ray crystallography. The ferromagnetic Co_3O_{14} triangular cluster core consists of three octahedrally oxo-coordinated Co^{II} ions sharing edges. According to the single-ion anisotropy and spin–orbit coupling usually assumed for octahedral Co^{II} ions, the appropiate exchange Hamiltonian to describe the ground-state properties of the isosceles triangular Co_3 spin cluster is anisotropic and is expressed as $\hat{H} = -2\sum_{\alpha=x,y,z}(J^{12}_{\alpha}\hat{S}_{1\alpha}\hat{S}_{2\alpha} + J^{23}_{\alpha}\hat{S}_{2\alpha}\hat{S}_{3\alpha} + J^{13}_{\alpha}\hat{S}_{1\alpha}\hat{S}_{3\alpha})$, where J_α are the components of the exchange interactions between the Co^{II} ions. To reproduce the INS data, nonparallel anisotropic exchange tensors needed to be introduced, which were directly connected to the molecular symmetry of the complex. The following range of parameters (value $\pm$ 0.5 cm^{-1}) was found to reproduce all experimental information while taking magnetostructural relations into account: $J^{12}_x = J^{13}_y = 8.6$ cm^{-1}; $J^{12}_y = J^{13}_x = 1.4$ cm^{-1}; $J^{12}_z = J^{13}_z = 10.0$ cm^{-1}; $J^{23}_x = J^{23}_y = 6.5$ cm^{-1} and $J^{23}_z = 3.4$ cm^{-1}.

Introduction

Polyoxometalates are complexes that can be described either 'top-down', as discrete fragments of metallic oxides or 'bottom-up', as condensed oxocomplexes. They are a rich and growing class of inorganic compounds[1] with interest both for their possible applications[2,3] and for their usefulness as model systems to understand the electronic properties of metal-oxides at the molecular level. This latter utility arises both from their ability to host delocalized electrons[4] and from their aptitude to encapsulate clusters of magnetic transition metal ions, while isolating them from the rest of the ions of the crystal. Further, the variety of possible highly symmetric structures exhibited by these magnetic clusters, together with the possibility to obtain clusters of larger and larger nuclearities, while maintaining the basic exchange-coupled units, have offered ideal systems to check the validity of the exchange Hamiltonians.[5,6] Thermodynamic techniques (magnetic and specific heat measurements) combined with Inelastic Neutron Scattering (INS) spectroscopy have been applied to polyoxometalates for investigations of magnetic exchange interactions with a high degree of success. Particularly, a detailed investigation, allowing for evidence of the anisotropic nature of the exchange interactions between Co(II) ions, has been performed on a family of polyoxotungstates of various nuclearities: From the simple Co^{II}_2

* Author to whom correspondence should be addressed. E-mail: juan.m.clemente@uv.es.
† Universitat de València.
‡ Universität Bern.
§ Institut Laue Langevin.

(1) *Chem. Rev.* **1998**, 98.
(2) Kozhevnikov, I. V.; *Chem. Rev.* **1998**, *98*, 171. Mizuno, N.; Misono, M. *Chem. Rev.* **1998**, *98*, 199. Sadakane, M.; Steckhan, E. *Chem. Rev.* **1998**, *98*, 219.
(3) Rhule, J. T.; Hill, C. L.; Judd, D. A.; Schinazi, R. F. *Chem. Rev.* **1998**, *98*, 327.
(4) Kozik, M.; Hammer, C. F.; Baker, L. C. W. *J. Am. Chem. Soc.* **1986**, *108*, 2748. Kozik, M.; Baker, L. C. W. *J. Am. Chem. Soc.* **1987**, *109*, 3159. Kozik, M.; Casañ-Pastor, N.; Hammer, C. F.; Baker, L. C. W. *J. Am. Chem. Soc.* **1988**, *110*, 1697. Kozik, M.; Baker, L. C. W. *J. Am. Chem. Soc.* **1990**, *112*, 7604. Casañ-Pastor, N.; Baker, L. C. W. *J. Am. Chem. Soc.* **1992**, *114*, 10384.
(5) Clemente-Juan, J. M.; Coronado, E.; Galán-Mascarós, J. R.; Gómez-García, C. J. *Inorg. Chem.* **1964**, *38*, 55−63.
(6) Clemente-Juan, J. M.; Coronado, E. *Coord. Chem. Rev.* **1999**, *361*, 193−195.

10.1021/ic048552w CCC: $30.25 © 2005 American Chemical Society
Published on Web 03/03/2005

moiety embedded in the salt K_8 $[Co_2(D_2O)W_{11}O_{39}]\cdot n\ D_2O$ (**Co**$_2$),[7] to nuclearities four, $K_{10}[Co_4(D_2O)_2\ (PW_9O_{34})_2]\cdot n\ D_2O$ (**Co**$_4$),[8,9,10] five, Na_{12} $[Co_3W(D_2O)_2(CoW_9O_{34})_2]\cdot n\ D_2O$ (**Co**$_5$),[11] and nine, $K_{16}[Co_9(OD)_3(D_2O)_6(HPO_4)_2(PW_9O_{34})_3]\cdot n\ D_2O$ (**Co**$_9$),[12] several studies about anisotropic magnetic interactions have been performed in the past decade.

The compounds **Co**$_2$, **Co**$_4$, and **Co**$_5$ were successfully studied by INS, while susceptibility, magnetization and specific heat measurements were used to cross-check the results. The magnetic exchange interactions between the Co^{II} ions, ferromagnetic in most cases, were found to be anisotropic. In some cases, axial anisotropy showed to be insufficient and a rhombic anisotropy was required to reproduce the experimental INS data. Notice that in all these systems the magnetic models assumed that each anisotropic exchange tensor is parallel to the main symmetry of the molecular cluster. In contrast to the previous clusters, the nonameric cluster, **Co**$_9$, has still to be properly analyzed. So far only magnetic properties were used to extract information on the exchange parameters. Still, due to its complexity a serious overparametrization problem appears that can only be overcome with a huge amount of independent high-quality experimental information and clear ground rules based on simpler systems. This makes the analysis of the title compound especially important as the nonameric cluster is formed by condensation of three **Co**$_3$ triangular units. Recently a polyoxoanion encapsulating a trinuclear Co unit has been studied by a detailed Inelastic Neutron Scattering (INS) experiment.[13] The polyoxoanion salt has the formula $Na_{12}[Co_3W(D_2O)(ZnW_9O_{34})_2]$ (shortly **Co**$_3$**W**) and can be viewed as a derivative of the salt $K_{10}[Co_4(D_2O)_2(PW_9O_{34})_2]\cdot n\ D_2O$ (**Co**$_4$), wherein one of the four Co(II) ions of the central rhomb-like cluster has been replaced by W(VI) (Figure 1). In this case, it was found that a parallel orientation of the anisotropic exchange tensors was unable to properly rationalize the experimental data, and an explicit consideration of the orientation of the local anisotropy axes determined by the geometry of the cluster was needed to be taken into account.

In this work we report a novel polyanion of formula $[(NaOH_2)Co_3(H_2O)(P_2W_{15}O_{56})_2]^{17-}$ (short **NaCo**$_3$) that contains a trinuclear Co_3 magnetic cluster deeply related with that of the **Co**$_3$**W** compound. In fact, this cluster is also derived from the rhomb-like cluster **Co**$_4$. However, while **Co**$_3$**W** contains an angular Co_3 cluster obtained by replacement of a Co situated in the short diagonal of the rhomb by W, **NaCo**$_3$ contains a triangular Co_3 cluster since one of the two Co's situated in the long diagonal of the rhomb has been replaced by Na^+ (Figure 1). Indeed, this new cluster should allow for examining how the different symmetry of the trinuclear cluster affects the orientation of the anisotropic exchange tensors.

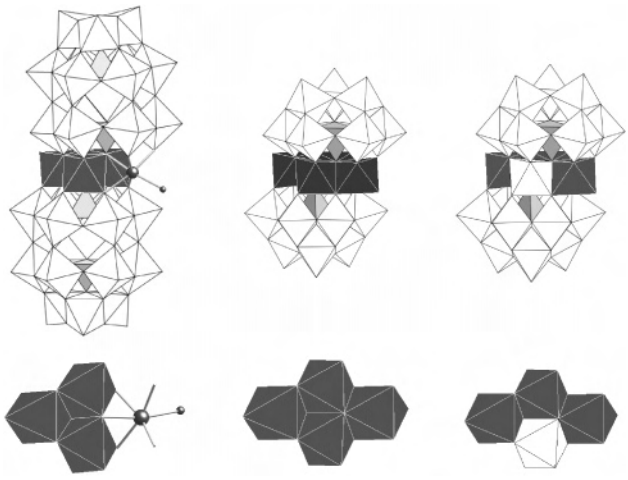

Figure 1. (top) Structures of Co the polyoxoanions (**Co**$_3$**W**) and (**NaCo**$_3$) (left and right) and comparison with the polyanion (**Co**$_4$) (center). (bottom) Geometries of the trinuclear Co(II) clusters encapsulated in the polyoxoanions **Co**$_3$**W** (left) and **NaCo**$_3$ (right) and their relation with the **Co**$_4$ rhomblike cluster.

2. Experimental Section

2.1. Synthesis. Approximately 10 g of **NaCo**$_3$ were obtained following a variation of a previously described procedure.[14,15] We used the following procedure: $Co(NO_3)_2\cdot 6H_2O$ (0.68 g, 2.34 mmol) was dissolved in 500 mL of 2 M NaCl deuterated aqueous solution and heated to 90 °C. α-$Na_{12}P_2W_{15}O_{56}\cdot 24H_2O$ (10.00 g, 2.26 mmol) (obtained as described[15]) was then added with vigorous stirring. The heating at 90 °C was continued for 20 min or until complete dissolution. A powder of a related compound $[(NaOH_2)_2Co_2(H_2O)(P_2W_{15}O_{56})_2]^{17-}$ **Na**$_2$**Co**$_2$ appeared first and was filtered away. Then, in the following 5−10 h, mixtures of **NaCo**$_3$ and **Na**$_2$**Co**$_2$ were formed and filtered. From the resulting solution, golden brown needles of the title compound were formed in 2−3 days (yield 30% approximately).

2.2. X-ray Diffraction. Crystals suitable for X-ray diffraction were obtained by synthesis in H_2O. A golden brown single crystal of dimensions $0.1 \times 0.1 \times 0.25$ mm was removed from the mother liquor and immediately cooled to 225(2) K under a nitrogen stream on a Nonius Kappa CCD diffractometer using a graphite monochromated MoK_α radiation source ($\lambda = 0.71073$ Å). Denzo and Scalepack[16] programs were used for cell refinements and data reduction. The structures were solved by direct methods using the SIR97[17] program with the WinGX[18] graphical user interface. The structure refinements were carried out with SHELX-97.[19] Multiscan

(7) Andres, H.; Aebersold, M.; Güdel, H. U.; Clemente-Juan, J. M.; Coronado, E.; Büttner, H.; Kearly, G.; Zolliker, M. *Chem. Phys. Lett.* **1998**, *289*, 224.
(8) Gómez-García, C. J.; Coronado, E.; Borrás-Almenar, J. J.; Aebersold, M.; Güdel, H. U.; Mutka, H. *Phys. B* **1992**, *180*−*181*, 238.
(9) Clemente-Juan, J. M.; Andres, H.; Aebersold, M.; Borrás-Almenar, J. J.; Coronado, E.; Güdel, H. U.; Büttner, H.; Kearly, G. *Inorg. Chem.* **1997**, *36*, 2244−2245.
(10) Andres, H.; Clemente-Juan, J. M.; Aebersold, M.; Güdel, H. U.; Coronado, E.; Büttner, H.; Kearly, G.; Melero, J.; Burriel, R. *J. Am. Chem. Soc.* **1999**, *121*, 10028.
(11) Andres, H.; Clemente-Juan, J. M.; Basler, R.; Aebersold, M.; Güdel, H. U.; Borrás-Almenar, J. J.; Gaita, A.; Coronado, E.; Büttner, H.; Janssen, S. *Inorg. Chem.* **2001**, *40*, 1943.
(12) Galán, J. R.; Gómez-García, C. J.; Borrás-Almenar, J. J.; Coronado, E. *Adv. Mater.* **1994**, *6*, 221.
(13) Clemente-Juan, J. M.; Coronado, E.; Gaita-Ariño, A.; Giménez-Saiz, C.; Chaboussant, G.; Güdel, H.-U.; Burriel, R.; Mutka, H. *Chem. Eur. J.* **2002**, *8*, 24, 5701−5708.
(14) Ruhlmann, L.; Canny, J.; Contant, R.; Thouvenot, R. *Inorg. Chem.* **2002**, *41*, 15, 3811−381.
(15) Contant, R. Early Transition Metal Polyoxoanions, 104−111.
(16) Otwinowski, Z.; Minor, W. DENZO-SCALEPACK, Processing of X-ray Diffraction Data Collected in Oscillation Mode. In *Methods in Enzymology, Volume 276, Macromolecular Crystallography, part A;* Carter, C. W., Jr., Sweet, R. M., Eds.; Academic Press: New York, 1997; pp 307−326.

Table 1: Comparison of Relevant Distances (Å), Bond Angles (deg) and Torsion Angles (deg) in the Compounds **NaCo**$_3$ and **Co**$_3$**W**[a]

		NaCo$_3$	**Co**$_3$**W**
distance (Å)	Co(1)−Co(2)	3.201(5)	3.170(2)
	Co(2)−Co(3)	3.188(5)	3.1728(14)
	Co(1)−Co(3)	3.184(5)	3.1828(19)
angle (deg)	Co(1)−O(58)−Co(2)	99.0(7)	96.5(4)
	Co(1)−O(50)−Co(2)	93.7(8)	101.6(4)
	Co(2)−O(57)−Co(3)	96.4(7)	101.9(4)
	Co(2)−O(50)−Co(3)	94.3(7)	101.9(4)
	Co(1)−O(63)−Co(3)	98.2(9)	96.6(4)
	Co(1)−O(50)−Co(3)	93.2(8)	101.6(4)
torsion angle (deg)	Co(1)−O(58)−O(50)−Co(2)	−175(1)	−168.4(5)
	Co(1)−O(63)−O(50)−Co(3)	172(1)	180
	Co(2)−O(57)−O(50)−Co(3)	−178.4(8)	166.9(4)

[a] The labeling is shown in Figure 3. In **Co**$_3$**W**, the positions Co(2)/Co(3) correspond to a disordered 50/50 occupation Co/W.

absorption corrections based on equivalent reflections were applied to the data using the program SORTAV.[20] All atoms were refined anisotropically with the exception of some disordered water oxygen atoms with occupancies of 0.5. Hydrogen atoms were not located. Further details of the crystal structure investigation can be obtained from the Fachinformationzentrum Karlsruhe, 76344 Eggenstein-Leopoldshafen, Germany, (fax: (+49)7247−808−666; e-mail: crysdata@fiz-karlsruhe.de) on quoting the depository number CSD-414656.

2.3. Magnetic Measurements. Variable-temperature susceptibility measurements were carried out in the temperature range 2−300 K on compacted powder molded from a ground crystalline sample of **NaCo**$_3$ on a magnetometer equipped with a SQUID sensor (Quantum Design MPMS-XL-5). The data were corrected for the diamagnetic contribution, which were estimated from the Pascal constants. Isothermal magnetization measurements at low temperature (2 K and 5 K) were performed up to a field of 5 T in the same apparatus.

2.4. Inelastic Neutron Scattering. INS spectra with cold neutrons were recorded on the time-of-flight spectrometer IN6 at the Institut Laue-Langevin (ILL) in Grenoble. The measurements were performed at 2, 10 and 30 K with incident wavelengths of $\lambda = 4.1$ Å.

The data processing involved the subtraction of a background spectrum measured on an empty aluminum container of the same size and calibration of the detectors by means of a spectrum of vanadium metal. Conversion of time-of-flight to energy and data reduction were done with the standard program INX at ILL. The spectra were treated further by using the free programs gawk and gnuplot.

3. Results

3.1. X-ray Diffraction. The structure of the salt $Na_{17}[(NaOH_2)Co_3(H_2O)(P_2W_{15}O_{56})_2]\cdot 41.5H_2O$ (shortly **NaCo**$_3$) was determined by X-ray crystallography. Crystallographic data and parameters are listed in Table 2.

This heteropolianion contains a sheet of three Co(II) ions and one Na^+, forming an oxo-aqua metallic core, $Co_3NaO_{14}(H_2O)_2$, which is sandwiched between two trivacant B-α-$[P_2W_{15}O_{56}]^{12-}$ subunits, as shown in Figures 2 and 3. The positions of the Co(II) and the Na^+ ions are unambiguously determined by the crystal structure determination and are not disordered as in the other existing example of a tricobalt sandwich type heteropolyanion $[Co_3W(D_2O)_2(ZnW_9O_{34})_2]$,$^{12-}$ (**Co**$_3$**W**[13]) in which only two positions of the central tetranuclear complex are fully occupied by Co, while the other two sites are each randomly occupied by one W atom and one Co atom. Despite that, the central tetranuclear complexes in **NaCo**$_3$ and **Co**$_3$**W** show quite identical geometries, as evidenced by the relevant bond distances and angles shown in Table 1.

Table 2: Crystal Data and Structure Refinement for the Salt $Na_{17}[(NaOH_2)Co_3(H_2O)(P_2W_{15}O_{56})_2]\cdot 41.5H_2O$

empirical formula	$H_{87}Co_3Na_{18}O_{155.50}P_4W_{30}$
formula weight	8805.69
temperature	225(2) K
wavelength	0.71069 Å
crystal system	triclinic
space group	$P\bar{1}$
unit cell dimensions:	a = 13.01200(10) Å
	b = 24.0312(2) Å
	c = 25.2498(3) Å
	α = 80.7875(4)°
	β = 82.9196(4)°
	γ = 85.9508(8)°
volume	7723.75(13) Å^3
Z	2
density (calculated)	3.786 Mg/m^3
absorption coefficient	22.757 mm^{-1}
F(000)	7780
crystal size	0.1 × 0.1 × 0.25 mm^3
theta range for data collection	1.79 to 29.17°
index ranges	$-17 \le h \le 17$, $-32 \le k \le 32$, $-34 \le l \le 34$
reflections collected	127722
independent reflections	40817 [R(int) = 0.1121]
completeness to θ = 29.17°	97.7%
absorption correction	semiempirical from equivalents
max. and min. transmission	0.103 and 0.008
refinement method	full-matrix-block least-squares on F^2
data/restraints/parameters	40817/129/1902
goodness-of-fit on F^2	0.977
final R indices [$I > 2\sigma(I)$]	R1 = 0.0975, wR2 = 0.2353
R indices (all data)	R1 = 0.1815, wR2 = 0.2772
largest diff. peak and hole	6.605 and −2.429 e.Å^{-3}

The crystal structure solution of **NaCo**$_3$ also confirms that the symmetry of the whole polyoxoanion is lowered to C_s as deduced by L. Ruhlmann et al. from the IR spectra of the compound[21] compared to the analogue polyoxoanion containing a tetracobalt sandwiched complex **Co**$_4$, which exhibits the symmetry C_{2h}.

3.2. Magnetic Measurements. Magnetic susceptibility data for a deuterated sample of **NaCo**$_3$ are shown in Figure 4(a), which plots $\chi_m T$ versus T at 0.1, 1, 2 and 4 T. At 0.1 T, $\chi_m T$ decreases upon cooling from 9.5 emu·K·mol^{-1} at 293 K down to 8.7 emu·K·mol^{-1} at 40 K, at which a round minimum is observed; then, it increases at lower temperatures

(17) Altomare, A.; Burla, M. C.; Camalli, M.; Cascarano, G.; Giacovazzo, C.; Guagliardi, A.; Moliterni, A. G. G.; Polidori, G.; Spagna, R. *J. Appl. Crystallogr.* **1999**, *32*, 115−119.
(18) Farrugia, L. J. *J. Appl. Crystallogr.* **1999**, *32*, 837−838.
(19) Sheldrick, G. M.; SHELX-97, an integrated system for solving and refining crystal structures from diffraction data, University of Götingen, Germany, 1997.
(20) Blessing, R. H. *J. Appl. Crystallogr.* **1997**, *30*, 421−426.
(21) Ruhlmann, L.; Canny, J.; Contant, R.; Thouvenot, R. *Inorg. Chem.* **2002**, *41*, 3811−3819.

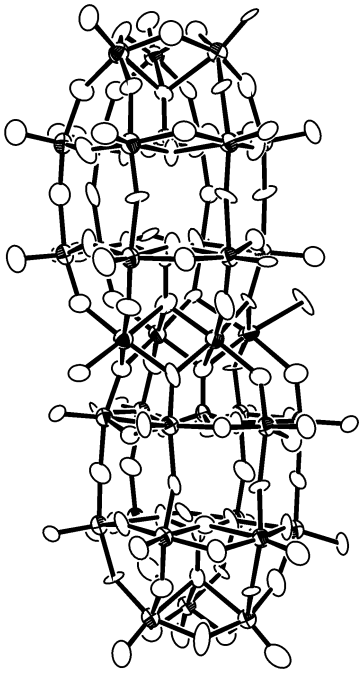

Figure 2. ORTEP plot of the anion showing 60% probability ellipsoids.

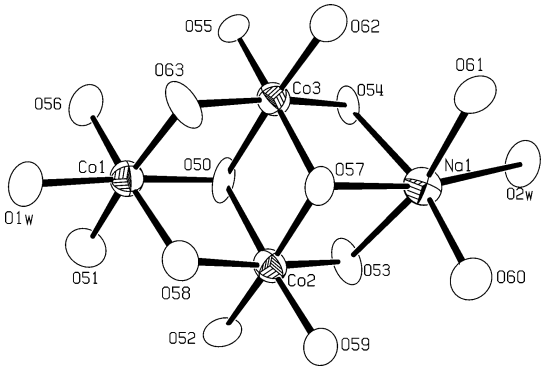

Figure 3. ORTEP plot of the encapsulated magnetic clusters showing 60% probability ellipsoids.

to reach a sharp maximum of 10.4 emu·K·mol^{-1} at about 6 K. The decrease from room temperature downward is due to spin−orbit coupling of Co^{II}, while the subsequent increase is indicative of ferromagnetic $Co^{II}-Co^{II}$ interactions within the trinuclear spin cluster. The low-temperature behavior (below 50 K) depends on the applied magnetic field. At 0.1 T, $\chi_m T$ reaches a maximum value of 10.4 emu·K·mol^{-1} at 6 K. At higher fields, the maximum shifts to higher temperatures and becomes lower and broader, so that at 2.5 T $\chi_m T$ has a maximum of 9 emu·K·mol^{-1} at 15 K. The dependence of the low-temperature isothermal magnetization on field at 2 and 5 K, from 0 to 5 T, is plotted in Figure 4(b).

3.3. Inelastic Neutron Scattering. Figure 5 shows the INS spectra of polycrystalline **NaCo**$_3$ with an incident neutron wavelength of 4.1 Å at three temperatures. The energy-transfer range between −3.8 and 4 meV is depicted with positive values for neutron-energy loss (right) and negative values for neutron-energy gain (left). The resolution is 110 μeV at the position of the elastic peak. At 2 K we observe a narrow band around 2.9 meV, that can be fitted with two very close-lying peaks, on the neutron-energy loss side. The

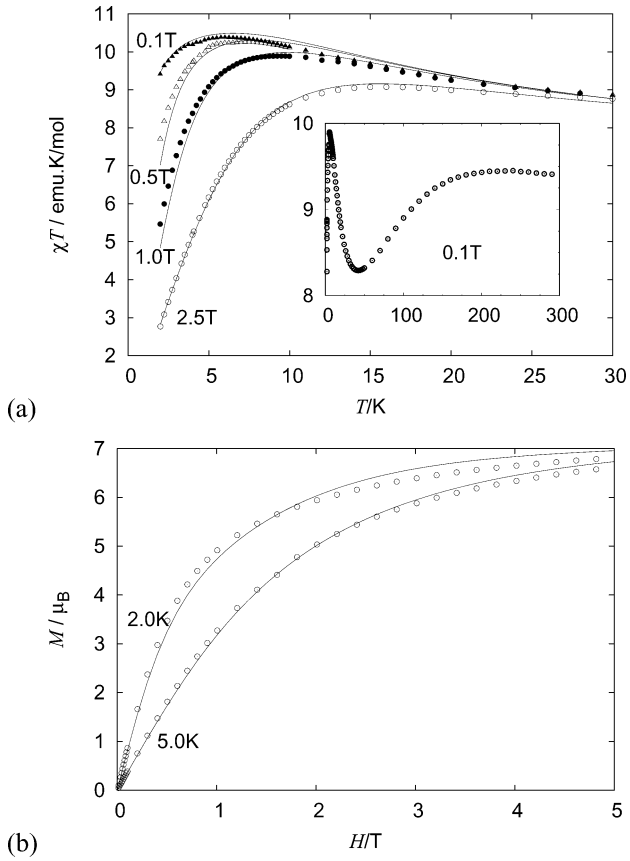

Figure 4. (a) Experimental $\chi_m T$ of a polycrystalline sample of **NaCo**$_3$ between 2 and 30 K at four different fields. (inset) Experimental $\chi_m T$ of the same sample at 0.1T in the temperature range 2−300K. (b) Isothermal magnetization of **NaCo**$_3$ at 2 and 5K. The solid lines represent the magnetic properties calculated by applying the Hamiltonian of eq 1 with the parameter set reported in eqs 6 and 8 (see 4.2).

transitions are labeled I, II. At higher temperatures, we can see a hot narrow band at 2.3 meV, that can also be fitted with two close-lying peaks. The corresponding gain transitions appear with rising temperature, but due to the low intensity and the high width it is not possible to resolve them properly and obtain quantitative intensities.

The least-squares fitting analysis in Figure 5 was performed by assuming a linear background and one Gaussian for each transition. The intensities derived from the least-squares fitting analysis are summarized in Table 3.

From the experimental data presented in Figure 5 and Table 3 we derive the energy diagram depicted in Figure 6. The cold transitions I and II coming from the ground level are indicated by full arrows, and hot transitions from the excited levels by broken arrows. Relative INS intensities were analyzed with a general formalism developed in refs 22 and 23 and integrated in the program package MAGPACK.

Taking into account the relative energies derived from the energy diagram (0, 0.65, 2.80 and 3.06 meV) and the temperature dependence of the peak intensities, this energy scheme is valid only if the four levels have equal degeneracy.

(22) Borrás-Almenar, J. J.; Clemente-Juan, J. M.; Coronado, E.; Tsukerblat, B. S. *J. Comput. Chem.* **2001**, *22*, 985.
(23) Waldmann, O. *Phys. Rev. B* **2003**, *68*, 174406.

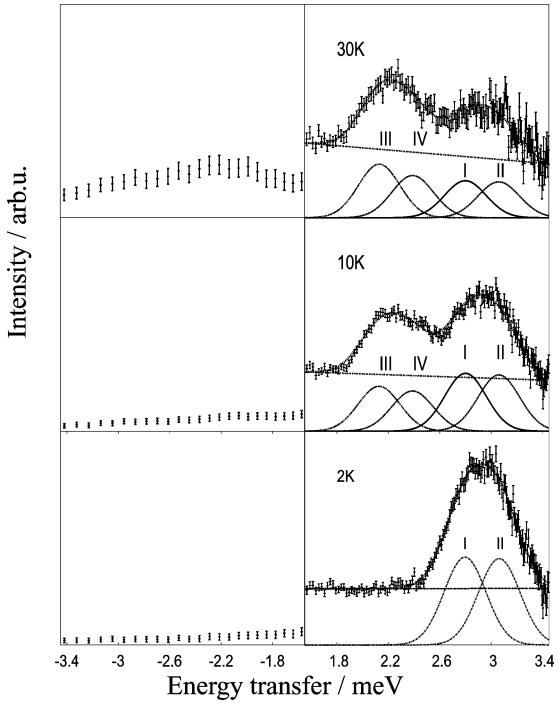

Figure 5. INS spectra of **NaCo**$_3$ at 2, 10 and 30K, measured on IN6 of ILL with an incident wavelength of $\lambda = 4.1$ Å. Dots with error bars are experimental data, straight lines are background signal, and Gaussians are fitted peaks. I and II are cold transitions, III and IV are hot transitions. Right: neutron-energy loss side. Left: neutron-energy gain side.

4. Discussion

4.1. Anisotropic Exchange Model. The $^4T_1$ high-spin ground state of distorted octahedral Co^{II} shows a first-order spin−orbit coupling and splits into six anisotropic Kramers doublets. At low temperature (below 30 K) only the lowest Kramers doublet is populated, so that the exchange interaction between two Co^{II} ions can be described by assuming a coupling between fully anisotropic Kramers doublets with effective spins of $^1/_2$. Expressing this spin anisotropy in terms of exchange anisotropy gives the effective exchange Hamiltonian for our Co^{II}_3 moiety:

$$\hat{H} = -2 \sum_{\alpha=x,y,z} (J^{12}_{\alpha}\hat{S}_{1\alpha}\hat{S}_{2\alpha} + J^{23}_{\alpha}\hat{S}_{2\alpha}\hat{S}_{3\alpha} + J^{13}_{\alpha}\hat{S}_{1\alpha}\hat{S}_{3\alpha}) \quad (1)$$

Generally, the operator involved in eq 1 does not commute with the total spin of the system. Therefore neither *S* nor *M* are good quantum numbers of the system, and the eigenfunctions of the trinuclear unit will be given by appropiate linear combinations of the $|(\hat{S}_2)SM\rangle$ basis functions:

$$\Psi_n = \sum_{S_2,S,M} a_n ((\hat{S}_2)SM)|(\hat{S}_2)SM\rangle \quad (2)$$

The structure of the full complex is shown in Figure 2, and the Co_3O_{13} subunit is depicted in Figure 3. The subunit is formed by three edge-sharing CoO_6 octahedra. As can be seen, each octahedron is connected with the other two, in an ideally equilateral fashion, but the symmetry is broken down to an idealized isosceles (C_s) triangle by the encapsulating polyoxometalate.

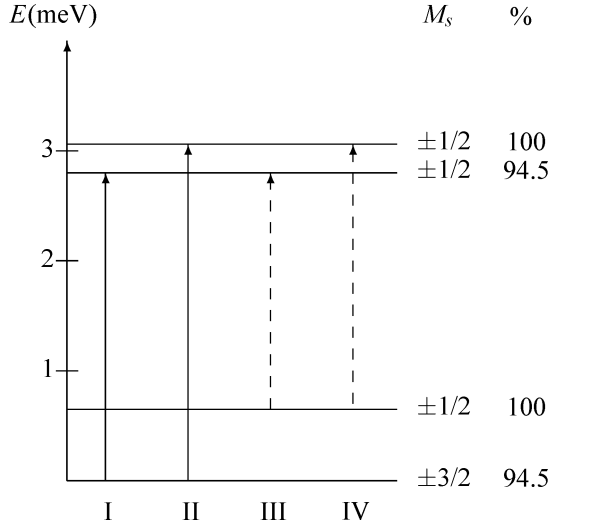

Figure 6. Experimental ground-state splitting. The cold transitions I and II coming from the ground level are shown with full arrows. The hot transitions coming from the excited level at 0.8 meV are shown with broken arrows. Each transition is experimentally observed but only in neutron-energy loss. Each level is labeled according to the M_s associated with the basis functions having the major contribution in the wave functions Ψ_n of the Co^{II}_3 moiety. This contribution, that is, the sum of the squared coefficients in the linear combination in eq 2, is given on the right.

Table 3: Experimental and Theoretical Energies (in meV) and Relative Intensities of the INS Transitions

	energy	2 K	10 K	30 K
III[exp]	2.13(1)	0.00	0.49(5)	0.60(4)
III[teo]	2.15	0.00	0.31	0.33
IV[exp]	2.39(1)	0.00	0.46(5)	0.48(4)
IV[teo]	2.43	0.00	0.31	0.32
I[exp]	2.80(1)	1.00(5)	0.66(3)	0.42(2)
I[teo]	2.80	1.00	0.66	0.42
II[exp]	3.06(1)	0.97(5)	0.65(3)	0.42(2)
II[teo]	3.05	0.99	0.66	0.42

In view of this geometry, we can distinguish two Co_{acute}−Co_{obtuse} (along the side of the rhomb) pairs, which are essentially equivalent and very similar to the analogous pairs in the angular trinuclear cluster **Co**$_3$**W**, and a unique Co_{obtuse}−Co_{obtuse} pair, along the short diagonal of the rhomb (Co2−Co3 in Figures 3 and 7). Here lies the main difference between **Co**$_3$**W** and **NaCo**$_3$: while the former is magnetically linear, the latter is magnetically triangular.

As seen in Figure 7, the orientations of the local anisotropy axes are supposedly parallel to the W−O bonds. This assumption relieves the unconquerable overparametrization that would arise if we would fully release the orientations of the local anisotropy axes. When the C_s symmetry of the system is taken into account, some relations among the exchange parameters J^{ij}_{α} appear naturally, namely

$$J^{12}{}_x = J^{13}{}_y,\ J^{12}{}_y = J^{13}{}_x,\ J^{12}{}_z = J^{13}{}_z,\ J^{23}{}_x = J^{23}{}_y \quad (3)$$

and J^{23}_z which is the only one to remain independent.

These considerations are of the same kind as those needed in the study of **Co**$_3$**W**.[13] Obviously, the relations are different, because of the different connectivity of the magnetic cluster. Furthermore, because of symmetry considerations in **NaCo**$_3$, we should expect J^{23}_z to be similar to J^{12}_y (and obviously J^{13}_x), while $J^{23}_x = J^{23}_y$ should be similar to $\{J^{12}_x, J^{13}_y, J^{12}_z, J^{13}_z\}$.

As $\mathbf{Co_3W}$ was magnetically linear, it could be described with a smaller number of independent parameters. Nevertheless, both compounds show an energy pattern with four energy levels. Being forced to fit an equally informative spectrum with a more complex model, we are faced with an overparametrization problem.

Besides these relationships, we can assume that the $Co_{acute}-Co_{obtuse}$ interactions are very similar to the analogous interactions in $\mathbf{Co_3W}$, which could be univocally determined. Likewise, some J components of the $Co_{obtuse}-Co_{obtuse}$ pair are expected to be an average of analogous ones in $\mathbf{Co_3W}$.

Thus, we limit the variations of their values to a minimum range around the original values. The details of these relations are included in eq 4.

$$J^{13}{}_x(\mathbf{NaCo_3}) \simeq J^{13}{}_x(\mathbf{Co_3W}) = 1.8\ \mathrm{cm}^{-1}$$
$$J^{13}{}_y(\mathbf{NaCo_3}) \simeq J^{13}{}_y(\mathbf{Co_3W}) = 11.0\ \mathrm{cm}^{-1}$$
$$J^{13}{}_z(\mathbf{NaCo_3}) \simeq J^{13}{}_z(\mathbf{Co_3W}) = 9.9\ \mathrm{cm}^{-1}$$
$$J^{23}{}_x(\mathbf{NaCo_3}) \simeq \frac{J^{13}{}_y(\mathbf{Co_3W}) + J^{13}{}_z(\mathbf{Co_3W})}{2} = 10.45\ \mathrm{cm}^{-1}$$
$$J^{23}{}_z(\mathbf{NaCo_3}) \simeq J^{13}{}_x(\mathbf{Co_3W}) = 1.8\ \mathrm{cm}^{-1} \qquad (4)$$

While without the use of information obtained from $\mathbf{Co_3W}$ an overparametrization problem arises, the inclusion of these considerations restricts the solution to an unique parameter range for $\mathbf{NaCo_3}$:

$$J^{13}{}_x = J^{12}{}_y = 1.4 \pm 0.5\ \mathrm{cm}^{-1}$$
$$J^{13}{}_y = J^{12}{}_x = 8.6 \pm 0.5\ \mathrm{cm}^{-1}$$
$$J^{13}{}_z = J^{12}{}_z = 10.0 \pm 0.5\ \mathrm{cm}^{-1}$$
$$J^{23}{}_x = J^{23}{}_y = 6.5 \pm 0.5\ \mathrm{cm}^{-1}$$
$$J^{23}{}_z = 3.4 \pm 0.5\ \mathrm{cm}^{-1} \qquad (5)$$

The calculated energies and intensities are in very good agreement with the experimental values (see Table 3). Within this full range of parameters the energy level scheme can be reproduced, but for the magnetic properties analysis we have selected the solution that gives the absolute minimum in this range, which is the following:

$$J^{13}{}_x = J^{12}{}_y = 1.36\ \mathrm{cm}^{-1}$$
$$J^{13}{}_y = J^{12}{}_x = 8.56\ \mathrm{cm}^{-1}$$
$$J^{13}{}_z = J^{12}{}_x = 10.08\ \mathrm{cm}^{-1}$$
$$J^{23}{}_x = J^{23}{}_y = 6.48\ \mathrm{cm}^{-1}$$
$$J^{23}{}_z = 3.36\ \mathrm{cm}^{-1} \qquad (6)$$

We can observe that the J tensor has two components of almost equal magnitude and larger than the third one. This smaller component corresponds to the direction perpendicular to the Co−O−O−Co plane, while the other two correspond to the two axes pointing toward the bridging oxo anions. The reduction of symmetry in the cases of exchange in the $Co_{acute}-Co_{obtuse}$ pairs can be attributed to the presence of a water molecule in the coordination sphere of Co_{acute}, in contrast with the exchange between the $Co_{obtuse}-Co_{obtuse}$ pair, where all oxygens are similar.

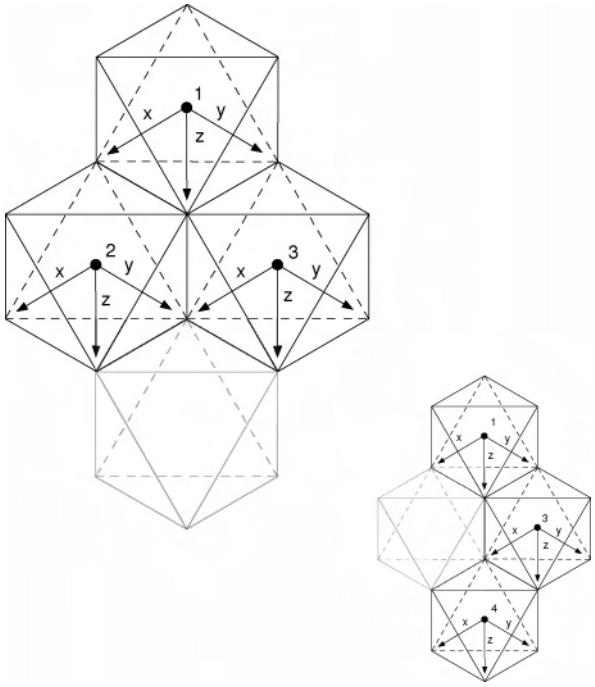

Figure 7. Assumed orientations of the local anisotropy axes, which have been chosen to point toward some of the oxo anions defining the octahedra of each site. The assumed C_s symmetry of the molecule applied to the spacial relations between the anisotropy axes defines the conditions in eqs 3 and 7. For the sake of comparison, the structure and orientations of the local anisotropy axes of the related compound $\mathbf{Co_3W}$ is depicted at the bottom right.

4.2. Analysis of the Magnetic Properties. To reproduce the low-temperature magnetic properties, the different g components associated with each center had to be taken into account. With this aim, the Zeeman terms were added to the Hamiltonian (eq 1), and the exchange parameters obtained from the INS analysis were conserved. In a first approximation, the three g tensors were considered to be parallel. Thus, with the only limitation $g_i^1 = g_i^2 = g_i^3$ ($i = x, y, z$), no solution was found after exploring the whole range of parameters. Hence, a more detailed consideration of the symmetry was again necessary to reproduce the experimental data. A solution was found with an orientation of the g tensors consistent with the one assumed for the J tensors:

$$g_x{}^1 = g_y{}^1, g_x{}^2 = g_y{}^3, g_x{}^3 = g_y{}^2 \qquad (7)$$

This model involves a large number of independent parameters. To relieve some of the overparametrization the fit was performed simultaneously over four $\chi_m T$ curves measured at different external magnetic fields, as seen in Figure 4(a). As the wave functions and eigenvalues of the magnetic cluster are accurately determined by INS, the differences observed in the χT curves at different magnetic fields can only be due to the Zeeman contributions.

An excellent fit can be found with the J set given in eq 6 and the following set of Landé parameters:

$$g_z^2 = g_z^3 = 6.77$$
$$g_x^2 = g_y^3 = 4.42$$
$$g_y^2 = g_x^3 = 5.47$$
$$g_x^1 = g_y^1 = 3.45$$
$$g_z^1 = 3.39 \quad (8)$$

Because of the relatively large number of independent g-parameters, there is no easy way to univocally determine them. In this sense, the g-parameter set should be seen just as a possible solution, and thus we will not try to interpret it.

Finally, the magnetization curves serve just as cross-checking, as they were not taken into account in any fit. We can see that the theoretical values are in good agreement with the experimental data, thus validating the model.

5. Conclusions

In this work we have studied the exchange interactions in a triangular Co^{II} cluster, **NaCo**$_3$, encapsulated by a polyoxometalate. The ferromagnetic and anisotropic exchange parameters found in **NaCo**$_3$ are within the range of those reported in the related compounds **Co$_3$W**, **Co$_4$** and **Co$_5$**. Most importantly, we have shown that in this cluster INS data are sensitive not only to the magnitude and anisotropy of the exchange parameters but also to the relative orientation of the exchange anisotropy axes. We have shown that the strategy for assigning anisotropy axes in **NaCo**$_3$ is equivalent to the one used in the angular trinuclear Co^{II} cluster **Co$_3$W** and equally successful. Moreover, magnetostructural analogies between the two compounds allowed us to select a unique solution for the title compound, showing the usefulness of serial studies to overcome the problem of overparametrization. The introduction of symmetry arguments in new related compounds as well as the possible reinterpretation of already studied compounds could lead to a better, general understanding of this family of Co^{II} polyoxometalates and, ultimately, of the anisotropic exchange interactions in Co^{II} systems.

Acknowledgment. Finantial support by the European Union (TMR Network MOLNANOMAG, contract HPRN-CT-1999-00012), the Spanish Ministerio de Educación y Ciencia (Projects BQU2002-01091 and MAT2004-3849) and the Swiss National Science Foundation are gratefully acknowledged. J.M.C.-J. and C.G.-S. thank the Ministerio de Ciencia y Tecnología for a RyC contract. A.G.A. acknowledges the Generalitat Valenciana for a predoctoral grant.

IC048552W